

JES FOCUS ISSUE ON ADVANCES IN MODERN POLYMER ELECTROLYTE FUEL CELLS IN HONOR OF SHIMSHON GOTTESFELD

Time Dependence of the Open Circuit Potential of Platinum Disk **Electrodes in Half Cell Experiments**

Uwe Reimer, ¹ ¹ ² Yun Cai, ¹ ² Ruiyu Li, ¹ Dieter Froning, ¹ and Werner Lehnert ¹

The time dependence of the open circuit potential under oxygen and air is characterized by half-cell experiments in the temperature range of 30°C to 80°C. The data is analyzed with the aid of a macroscopic model that captures the effect of a coupled reaction of platinum surface oxidation and the oxygen reduction reaction. The aim of the model is to facilitate an understanding of the principle reactions from an engineering perspective. Two modeling approaches, namely 'gas electrode' and 'flooded electrode', are compared. It can be shown that the difference between the theoretical Nernst potential and open circuit potential can be described by two major effects: gas solubility in the electrolyte and platinum surface oxidation. The fact that platinum surface oxidation does not lead to a 'fully oxidized surface' has strong implications for the design of accelerated stress tests, which is briefly discussed.

© The Author(s) 2019. Published by ECS. This is an open access article distributed under the terms of the Creative Commons Attribution 4.0 License (CC BY, http://creativecommons.org/licenses/by/4.0/), which permits unrestricted reuse of the work in any medium, provided the original work is properly cited. [DOI: 10.1149/2.0121907jes]

Manuscript submitted December 7, 2018; revised manuscript received February 8, 2019. Published March 26, 2019. This paper is part of the JES Focus Issue on Advances in Modern Polymer Electrolyte Fuel Cells in Honor of Shimshon Gottesfeld.

Polymer electrolyte membrane fuel cells are highly efficient energy converters. The introduction of polymer membranes allowed for very compact designs with a high power density and thin catalyst layers. The main material for these catalysts is nanometer-sized platinum on carbon supports. The total amount of platinum should be as low as possible in order to decrease unit costs. On the other hand it is known that several degradation processes lead to the loss of the catalyst. 1-3 These processes partly occur in conditions in which the cell is in the range of the so-called open circuit voltage (OCV). Every fuel cell usually goes through a time period with zero electrical load during start up and shut down. During this time, the cell is at its open circuit voltage. In fuel cell experiments it is frequently observed that the OCV value is not in fact a fixed number. The value may vary between different single cells, manufacturer and operating conditions (especially humidification). Furthermore, after switching to OCV condition the cell voltage changes by several mV over several hundred seconds and a value that is truly independent of time is never observed. With respect to degradation and long term stability, it is important to understand the effects that occur at the platinum surface under these conditions.

A recent publication by Cherevko et al.⁴ summarizes the effects of Pt surface oxidation and reduction. It can be concluded that the overall process is complex and not yet fully understood, but the main mechanism seems to be clear. Under OCV conditions, an oxide layer forms at the surface of Pt electrodes. It can be argued that this will lead to a mixed electrode potential which in turn can explain the deviation from the thermodynamic potential.^{5–8} On the other hand Zhang et al.⁹ have observed in PEFC experiments that the OCV value depends on the thickness of the Nafion membrane. They measured the hydrogen cross-over and showed that the resulting overpotential of hydrogen oxidation at the cathode side can be used to explain the observed OCV values. In general, the mismatch of the OCV value and thermodynamic potential is explained by a combination of three different effects. 9-16 Firstly, the permeability of the polymer membrane leads to a small cross-over of hydrogen and oxygen to the opposite side of the membrane. This changes the local concentrations at the catalyst surface and is frequently referred to as mixed potential. Secondly, technical catalyst layers consist of a mixture of different materials. Additionally, the platinum catalyst is in a reduced state on the hydrogen side and in a (partially) oxidized state at the oxygen side. This can also be understood as a contribution from the mixed electrode potential. Thirdly, the catalyst is in fact covered by a thin film of water or, more precisely, a matrix of Nafion/water and eventually other polymers. Thus,

gas solubility within this thin liquid film must be taken into account

lifetime of PEFCs, because this potential window is passed for each

The state of the catalyst under OCV has a significant impact on the

in order to obtain realistic concentrations at the catalyst surface.

of catalysts, several accelerated stress tests have been developed. 17,18 These tests are suitable for material screening. For lifetime predictions the interpretation of the results is difficult because the applied voltage frequently exceeds the range that is observed during fuel cell operation and enters a range in which different oxidation reactions at the catalyst may occur. The topic of platinum surface oxidation is also interesting for the modeling of fuel cells and related electrode processes. In many engineering models, the voltage of an operating fuel cell is calculated from the thermodynamic potential of the Nernst equation, with the kinetic and transport losses subsequently subtracted. 10,19-21 Unfortunately, the calculated Nernst voltages almost never reflect the observed open circuit voltages. This offset must be compensated (intentionally or unintenionally) by some of the model parameters in order to match the experimental polarization curves. The overall effect is that the kinetic model parameters may differ by several orders of magnitude if taken from different sources.10

The main objective of this work is to implement the knowledge that has been generated in recent years regarding the effect of platinum surface oxidation. With this aid, the process of fuel cell shut-down is experimentally characterized with a model system of a polycrystalline Pt disk within an electrochemical half-cell. This setup avoids the aforementioned effect of hydrogen cross-over in fuel cells and offers insight into the time-dependence of the electrode potential. The experiment is complemented by a modeling approach that takes into account the kinetic process of platinum surface oxidation and gas solubilities in the liquid electrolyte. The model is targeted at an engineering level, which would be suitable for aiding the evaluation of stress tests. It may also improve understanding of the open circuit voltage of fuel cell like devices.

Background

The overall fuel cell reaction is shown in Equation 1.

$$0.5 O_2 + H_2 \rightleftharpoons H_2 O$$
 [1]

Drawing on standard textbooks, the equilibrium voltage of E^0 1.23 V can be easily obtained. Strictly speaking, this is only true

 $^{^{}l}$ Forschungszentrum Jülich GmbH, IEK-3: Electrochemical Process Engineering, 52425 Jülich, Germany

²Modeling in Electrochemical Process Engineering, RWTH Aachen University, 52056 Aachen, Germany

start up and shut down process. In order to assess the long term stability

⁼These authors contributed equally to this work.

zE-mail: u.reimer@fz-juelich.de; y.cai@fz-juelich.de

Table I. Half-cell reactions and corresponding potentials based on thermodynamic data for 25°C and 101325 Pa.

Number	r Reaction	E^0 / V	Reference
1	$0.5 O_2 + 2 H^+ + 2 e^- \rightleftharpoons H_2O$	1.23	27
2	$PtOH^+ + H^+ + 2 e^- \rightleftharpoons Pt + H_2O$	1.20	27
3	$Pt^{2+} + 2 e^- \rightleftharpoons Pt$	1.18	4,27
4	$PtO_2 + 2 H^+ + 2 e^- \rightleftharpoons PtO + H_2O$	1.01	4,27
5	$PtO_2 + 4 H^+ + 4 e^- \rightleftharpoons Pt + 2 H_2O$	1.00	27
6	$PtO_2 + 2 H^+ + 2 e^- \rightleftharpoons PtO(hydr.) +$	1.05	4,26
	H_2O		
7	$0.5 \text{ PtO}_2(\text{hydr.}) + 2 \text{ H}^+ + 2 \text{ e}^- \rightleftharpoons 0.5 \text{ Pt} + \text{H}_2\text{O}$	1.00	26
8	$PtO(hydr.) + 2 H^+ + 2 e^- \rightleftharpoons Pt + H_2O$	0.98	4,26

under standard conditions and if the catalyst on both sides is the same (pure platinum). The thermodynamic value should be corrected for the presence of platinum surface oxide, but the oxidation process of platinum is highly complex and, at present, not completely understood.⁴ Depending on the specific conditions and time scale, many different oxide species may be formed that differ in terms of film thickness and electrochemical behavior.^{4,22–26} A deeper discussion of this effect can be found in the work of Cherevko et al.⁴ From the thermodynamic data, it becomes clear that several surface oxides may be present at OCV conditions. Table I gives a short overview that is late used as a starting point for the model derivation. The underlying idea is that in the range of the open circuit voltage, two reactions take place simultaneously at the surface of the cathode electrode: the formation of water and platinum surface oxidation.

The state of the platinum surface species can be characterized by cyclic voltammetry (CV).^{28–34} Figure 1 shows a typical CV for platinum under nitrogen and oxygen saturation. The oxidation peak between 0.9 V and 1.2 V is identical for nitrogen and oxygen saturation. For values below 0.9 V, the CV differs. In the case of nitrogen, a small reduction peak occurs at roughly 0.8 V, while the CV curve stays at zero net current, because only electric double layer charging takes place at the electrode surface. Below 0.4 V, the two characteristic hydrogen peaks are present. In the case of oxygen, the reduction peak at 0.8 V is much larger. Beyond that, the CV curve is shifted downwards because, at the electrode, the oxygen reduction reaction takes place.

In Figure 1, it can clearly be seen that the peak of surface oxidation is not symmetrical. The surface reduction process is shifted to significantly lower potential. This effect can be explained by the formation of different surface oxide species. In the case of nitrogen-saturated electrolyte, several adsorption and surface oxidation steps have been described. 4.28-35 The surface of platinum seemingly undergoes different states that involve the initial adsorption of oxide or hydroxyl species, partial surface layer oxidation and the rearrangement of surface layers. This leads to a broad distribution of several wide peaks

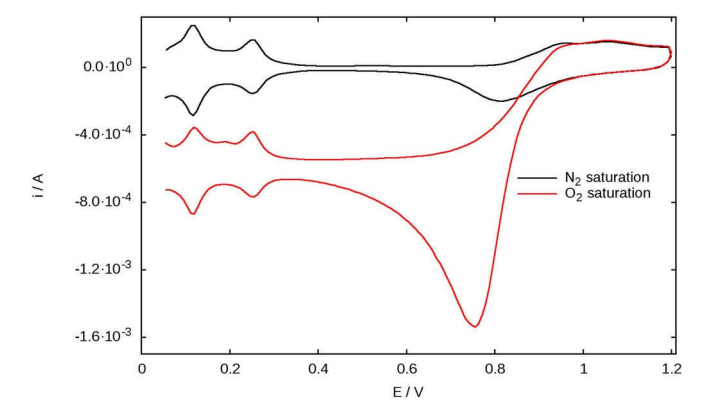


Figure 1. Cyclic voltammogram for a three electrode cell with a Pt disk electrode in 1 M H_2SO_4 against RHE at T = 30°C.

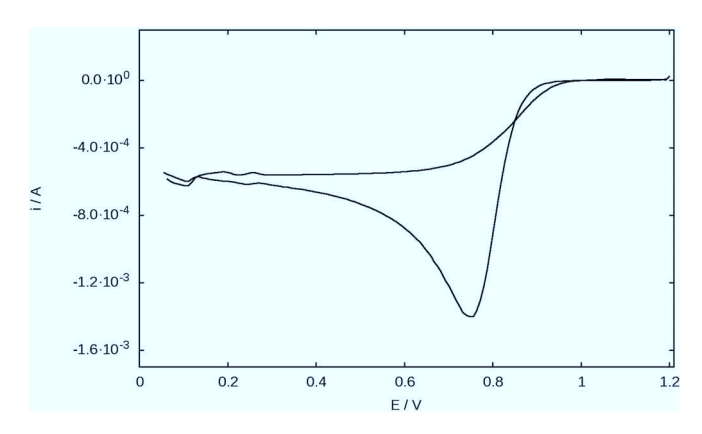


Figure 2. The resulting graph from the subtraction of the cyclic voltammograms of nitrogen and oxygen from Figure 1.

at the onset of surface oxidation, which are usually hard to resolve in cyclic voltammogrames. ^{28–30} It can also be noticed that there is a significant difference between nitrogen and oxygen saturation. In Figure 2 the cyclic voltammograms of nitrogen and oxygen are subtracted and the graph shows the difference between them. Both curves are identical for potentials above 0.9 V. Interestingly, this is precisely the range of the open circuit voltage of fuel cells. Below this value, the curve for oxygen shows a decline due to the oxygen reduction reaction. The largest deviation can be seen for the strong platinum surface reduction peak just below 0.8 V, which is very prominent in case of oxygen saturation.

It may be true that the real process of surface oxidation and the composition of the platinum surface is not completely understood,⁴ but there are some convincing suggestions that are summarized in the following. One of the earliest suggestions was published by Conway et al.^{28–30,35} and Anastasijević et al.³⁶ A six-step reaction mechanism is proposed that starts with the adsorption of OH species to the Pt surface. The following steps include the restructuring and further oxidation of the Pt surface layer. Three characteristic values were identified in the CV: the onset of oxidation at 0.89 V and two small oxidation peaks (within a broader region) at 0.95 V and 1.05 V.^{28,30} Nagy and You³⁷ proposed a three step mechanism. Step 1 includes the initial adsorption of OH at 0.9 V. Step 2 describes the surface reconstruction and further oxidation at ≤ 1.20 V. Step 3 summarizes further oxidation of the platinum surface at > 1.20 V. Jerkiewicz et al.³¹ proposed a twostep mechanism, where in step 1 the adsorption of half a monolayer of oxygen takes place in the range of 0.85 < E < 1.10 V. Step 2 describes adsorption of the second half monolayer of oxygen and the further oxidation of the platinum surface layer to PtO in the range of 1.20 $\leq E \leq$ 1.40 V. Drnec et al.^{32,33} also proposed a two-step mechanism for Pt(111) surfaces. Step 1 is the formation of Pt surface oxide which sharply peaks in the CV at 1.05 V. In step 2, further oxidation and restructuring of surface occurs in the range of ≥ 1.15 V. A detailed analysis of the oxidation of Pt(111) surfaces was formerly provided by Gómez-Marín et al.34 Holby and Morgan developed a comprehensive model for platinum surface oxidation³⁸ with the goal of characterizing platinum dissolution. The model is based on the preceding work of Darling and Meyers.³⁹ With the aid of the model, the effect of oxide roughening in cycling experiments is explained. The model is also capable of correctly reproducing the shape of cyclic voltammorgrams in a nitrogen atmosphere.

Within the scope of this work, the proposed surface oxidation mechanisms $^{4,28-35}$ are summarized in two significant steps that are common for all cited models. The first one describes the adsorption of oxygen or hydroxyl species to the surface of platinum at a potential of ≈ 0.9 V. The second merges subsequent oxidation and platinum surface rearrangement steps that take place with further increasing potential. The necessity to incorporate more oxygen per platinum surface atom leads to a restructuring of the outermost platinum layers. Figure 3 summarizes the overall effect.

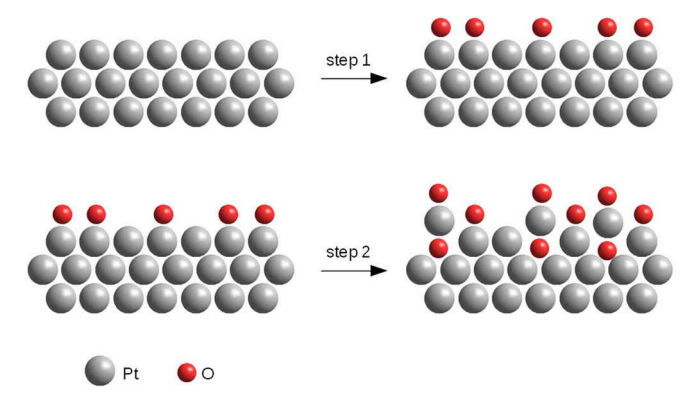


Figure 3. Schematic representation of platinum surface oxidation. Step 1: initial oxygen or hydroxyl adsorption in the range of 0.90 V-1.10 V. Step 2: further oxidation and surface reconstruction at $\geq 1.15 \text{ V}$.

In the literature noted above, the mechanism of platinum surface oxidation is investigated as a function of potential. In the case of the OCV of a polymer electrolyte fuel cell, the potential results from the kinetics of the surface reaction. It was suggested in an earlier work by Hoare et al. ⁴⁰ that under OCV conditions, an incomplete adsorption layer of PtO should be observed. In the presented experiments, the platinum surface is first transformed into its reduced state at 0.5 V. Then, the kinetics of surface oxidation can be derived by observing the open circuit potential as a function of time.

Experimental

Setup.—The experimental setup consists of a special cell, typically with a three-electrode arrangement, as discussed by Weissbecker et al. 41,42 A polycrystalline Pt disk serves as the working electrode, with a geometric area of 2.54 cm². The counter-electrode is a Pt mesh. A reversible hydrogen electrode is used as the reference electrode and connected to the cell by a Luggin capillary. The complete device is kept at a constant temperature, with a reflux condenser applied to maintain the water content of the electrolyte at elevated temperatures. At the start of the experiments, the platinum disk electrode was polished with alumina paste (Buehler) with a particle size of 5 μm, 1 μm and 0.05 μm, respectively. Then, a cleaning step with ethanol and distilled water was applied in an ultrasonic cleaner for 15 min. Finally, the disk was dried with a high-pressure air flow. The electrolyte, 1 M sulfuric acid, is prepared by diluting 98 wt% H₂SO₄ (AR regent). The glassware was deep-cleaned, as described by Garsany et al. 43 Before filling in the electrolyte, the glassware is rinsed several times with ultra-pure water and, subsequently, with electrolyte solution. After assembly, the cell was filled with 165 mL electrolyte solution and heated to the required temperature. All electrochemical measurement were performed using an Autolab potentiostat PGSTAT302N (Metrohm).

Some experiments were repeated using a standard rotating disk electrode (PINE Research/ E3 series). It showed reasonable agreement, but in the case of the rotating disk electrode, the signal was not particularly stable over the 1600 s timeframe and the reproducability was suboptimal. The main problems appeared to be the maintenance of constant temperature and constant gas saturation over this long time period. The cell described above showed much better reproducibility and long-term stability for these kinds of experiments.

Measurement procedure.—At the beginning of each measurment cycle the cell was purged for 60 min with nitrogen at a gas flow rate of 100 mL min⁻¹. Subsequently, cyclic voltammetry was applied in the potential range between 0.05 V and 1.20 V for eight cycles with a scan rate of 50 mV s⁻¹ to verify a clean electrode surface. After switching the gas supply to oxygen for another 60 min, the CV cycles were recorded again.

The time-dependence measurement of the OCV was always performed twice. First, the platinum surface was transformed into it's reduced state by the application of linear sweeping voltammetry in the range of 1.1 V to 0.4 V (at 50 mV s $^{-1}$). After that the OCV of the cell was recorded for 1600 s. Some operating conditions have been selected at random for additional repeated measurements in order to assure good reproducibility of the data.

Modeling Approach

Phenomenological model of the combined electrode.—The oxidation of the platinum surface is a reaction that involves many different intermediate steps. Within the scope of this work, the overall process is summarized by the growth of a single monolayer, as shown in the upper part of Figure 3. This assumption is motivated by the goal of finding a consistent description that contains a minimum number of fitting parameters. It is based on the suggestions of Hoare et al. 40 concerning the formation of a monolayer of oxide species. For the summary reaction, we chose reaction number 8 from Table I.

A first order rate reaction is used to model the time-dependence of the platinum surface species, as shown in Equation 2 and 3. Here, k is the reaction rate and t is the time. The concentration of platinum surface species can be understood as the surface coverage (or surface fraction) S of these species. The equations have been chosen to reflect the fact that at t=0, the surface is covered with Pt, and therefore Equation 2 yields $S_{\text{Pt}}=1$ for t=0.

$$S_{Pt} = \exp(-kt)$$
 [2]

$$S_{PtO} = 1 - \exp(-kt)$$
 [3]

In the next step the surface coverage (or, respectively, the normalized surface concentration) must be related to the voltage. This is achieved by applying the Nernst Equation. A challenge arises in deriving a formulation that incorporates two coupled reactions at the same electrode. It is assumed that at the working electrode, two cathodic half-cell reactions occur at the same time: the oxygen reduction reaction (Equation 4) and platinum surface oxidation (Equation 5). (Note that the reactions are written in the direction that the electrons are received, which follows from the definition of a cathodic process.) The incorporation of the oxygen reduction reaction is a major difference to the model by Holby and Morgan. ³⁸

$$0.5 O_2 + 2 H^+ + 2 e^- \rightleftharpoons H_2 O$$
 [4]

$$PtO + 2H^+ + 2e^- \rightleftharpoons Pt + H_2O$$
 [5]

The potential of the working electrode is measured against the reference hydrogen electrode, which is described by the anodic half cell reaction in Equation 6.

$$H_2 \rightleftharpoons 2H^+ + 2e^-$$
 [6]

The Nernst Equation for the combination of Reactions 4 and 6 is well known for it's description of fuel cell processes.

$$E_{H2O}(T) = E_{H2O}^{0}(T) - \frac{RT}{2F} \left(\ln X_{H2O} - \ln X_{H2} - 0.5 \ln X_{O2} \right)$$
 [7]

In the same way, Equation 8 is obtained for the surface oxidation of platinum as a combination of Reactions 5 and 6.

$$E_{PtO}(T) = E_{H2O}^{0}(T) - E_{PtO}^{0}(T) - \frac{RT}{2F}$$

$$(\ln X_{Pt} + \ln X_{H2O} - \ln X_{PtO} - \ln X_{H2})$$
[8]

The Nernst Equation for the combined electrode is obtained with the aid of the following arguments.

• Both half-cell Reactions 4 and 5 occur at the same electrode. Therefore, they must be at the same potential. This point is supported by the fact that the half-cell potentials of these two reactions are usually found to be in the same narrow range, while taking into account that the platinum surface may contain a mixture of different species.

- Both half-cell Reactions 4 and 5 are coupled through the concentration of protons. Furthermore, the surface oxidation state of platinum will influence the catalysis of the oxygen reduction reaction. Therefore, the logarithmic terms of the two Nernst equations are combined.
- The activity of water and platinum is assumed to be one. Therefore, the logarithmic terms for these two species are neglected.
- The standard potential of half-cell Reactions 4 and 5 cannot in fact be measured independently. Thermodynamic data is readily available for $E^0_{H2O}(T)$. It can be assumed that the presence of surface oxides may induce a contribution from mixed potential $E^0_{mix}(T)$.

The present work reports half cell measurements. Therefore, only the potential of the cathode is considered and we use in the following the term open circuit potential (OCP) instead of OCV, because the term voltage refers to the potential difference between two electrodes (e.g. of a fuel cell). According to the considerations above the open circuit potential $E_{OCP}(T)$ can be described by the following equation.

$$E_{OCP}(T) = E_{H2O}^{0}(T) - E_{mix}^{0}(T) + \frac{RT}{2F}$$

$$(\ln X_{PtO} + \ln X_{H2} + 0.5 \ln X_{O2})$$
[9]

In order to obtain a time-dependent expression, the mole fraction of PtO can be substituted in Equation 9 by the surface coverage from Equation 3.

$$E_{OCP}(T,t) = E_{H2O}^{0}(T) - E_{mix}^{0}(T) + \frac{RT}{2F} \left(\ln(1 - e^{-kt}) + \ln X_{H2} + 0.5 \ln X_{O2} \right)$$
[10]

In the absence of oxidized platinum species, Equation 9 reduces to the well-known form for fuel cells in the presence of liquid water. If the surface is 'fully' oxidized, it is independent of the surface coverage of PtO and the resulting Nernst equation would be equal to the fuel cell reaction with an additional term for the mixed potential E^0_{mix} , which accounts for the fact that on the anode side, the catalyst is Pt and on the cathode side is (partly) oxidized platinum.

The validity of Equation 10 is primarily restricted by two factors. Firstly, the equation was derived under the assumption of a summary surface oxidation reaction that actually involves several steps. Therefore, one single term for the surface coverage is a simplification. Secondly, the model assumes a complete oxidation of the platinum surface for $t \to \infty$. It is known from the literature that a higher fraction of surface oxides is only reached at much higher potentials. Therefore, the model will overestimate the resulting potential for large values of

Calculating the Nernst potential.—In the literature can be found several ways to calculate the Nernst potential of a fuel cell. All of them are more or less equivalent, as was shown by Reimer et al. ¹⁰ Within this work, the following two approaches will be used: the model assumption of the 'gas electrode' and that of the 'flooded electrode'. For both model approaches it is assumed that liquid water is in equilibrium with the gas phase. If two phases are in equilibrium, according to basic thermodynamics, the chemical potential for the substance is identical in each phase. For water, it can be assumed that the activity in the liquid phase is one, while the activity in the gas phase can be calculated from the vapor pressure curve. For oxygen and hydrogen, the activity in the gas phase can be obtained directly from the reduced partial pressure (i.e., the mole fraction $X = p/p^0$). The activity in the liquid phase is reflected by the gas solubilities.

For the 'gas electrode', the gas phase concentrations are used for the calculation. This is a common approach in fuel cell engineering. As liquid water is present, the dry gas concentrations must be corrected for the equilibrium water vapor content. The equilibrium water vapor pressure is obtained from the Antoine Equation $11.^{44}$ Then, the mole fraction of water vapor X_{vap} is calculated by means of Equation 12.

$$\log p = 4.6543 - \frac{1435.264}{T - 64.868}$$
 [11]

Table II. Specific solubility parameters for oxygen and hydrogen (T = 273 K to 353 K) at ambient pressure.⁴⁵

Hydrogen
-48.1611
55.2845
16.8893

$$X_{vap} = 10^{\log p} \cdot (10^5 Pa) / (101325 Pa)$$
 [12]

For the 'flooded electrode', the species concentration at the catalyst interface is calculated from solubility data. For the three-electrode cell, this is a straight-forward assumption, as the gas phase is not in direct contact with the electrodes. For fuel cells, this is equivalent to the assumption of a thin liquid layer that completely wets the catalyst surface. The mole fraction of dissolved oxygen and hydrogen in the temperature range of 273 K to 353 K can be obtained by Equation 13. 45 The specific solubility parameters are given in Table II.

$$\ln X_i = a_1 + a_2 \, \frac{100 \, K}{T} + a_3 \, \ln \left(\frac{T}{100 \, K} \right) \tag{13}$$

The temperature-dependence of $E_{H2O}^0(T)$ is obtained from a linear interpolation of thermodynamic data⁴⁶ (Equation 14).

$$E_{H2O}^{0}(T) = -\frac{1}{2F} \cdot (-237141 \, J \, mol^{-1} + 159.75 \, J \, mol^{-1} K^{-1} \cdot (T - 298 \, K))$$
 [14]

Figure 4 shows the measured open circuit potentials in the temperature range from 30°C to 80°C. It can be seen that the model assumption of the 'flooded electrode' yields a Nernst potential, which is much closer to the experimental data. On the other hand, the model of the 'gas electrode' yields a better match of the temperature dependence.

Fitting procedure.—The time-dependence of the open circuit potential is described by Equation 10. This equation contains two fitting parameters: the mixed potential E^0_{mix} and kinetic rate constant k. Both are obtained for each temperature by a manual fitting method from the experimental results. The model always uses a time offset of 30 s compared to the experiment. It was unclear whether this delay was caused exclusively by the data acquisition software. Another explanation could be the fact that the growth of the assumed monolayer is delayed by some previous adsorption reaction steps that are not covered by this coarse assumption. The following routine was used to obtain the model results.

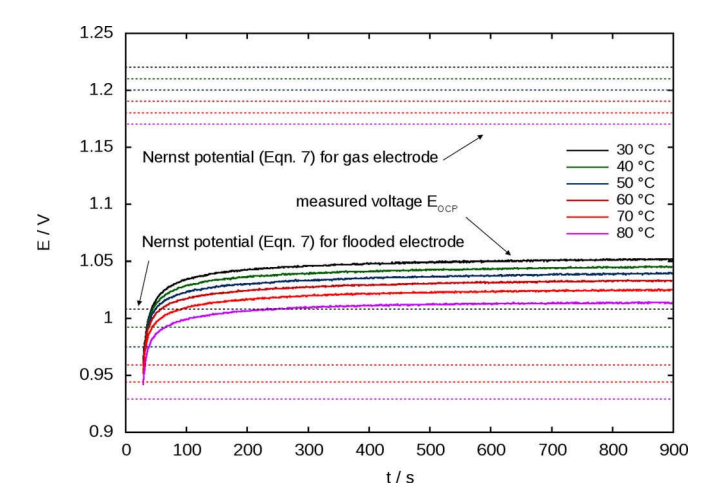


Figure 4. Open circuit potential of a Pt disk electrode in 1 M H_2SO_4 saturated with oxygen against RHE. The dashed lines represent the theoretical Nernst potential for liquid water formation calculated with gas phase concentrations (upper part) and gas solubilities (lower part).

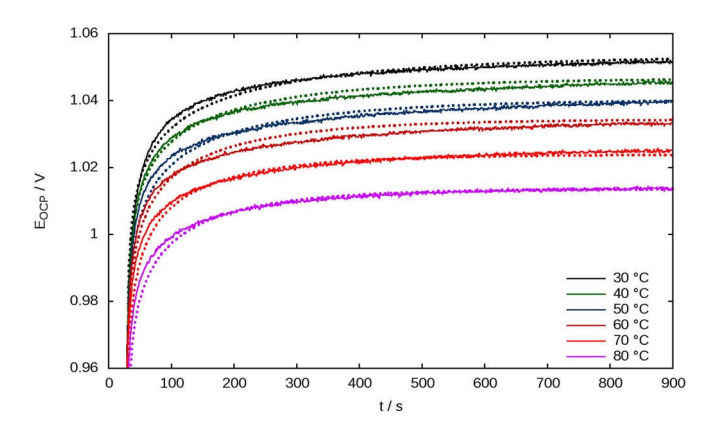


Figure 5. Time-dependence of the open circuit potential of Pt in 1 M H_2SO_4 in a pure oxygen atmosphere. Straight lines = experiment and dotted lines = model from Equation 10.

- 1. Choose a value for E_{mix}^0 and k as the starting point.
- 2. Change E_{mix}^0 until roughly the correct potential is obtained.
- 3. Change *k* until the correct shape of the curve is represented.
- 4. Adjust E_{mix}^0 to fit the curve.
- Vary k in order to explore the range of uncertainty. A reasonable fit is considered within a range of ±2 mV.

The procedure is fairly robust, because only k affects the shape of the curve. The fact that there are two parameters obtained from one curve leads to an additional degree of freedom. It can be shown that within a certain range, several parameter combinations may yield a good curve fitting. In order to estimate the range of uncertainty, the value of E_{mix}^0 was fixed and k was varied, as described above. Therefore, the values for the uncertainty of k in the resulting plots are overestimated and should be considered to be a summary of the contribution of k and E_{mix}^0 .

Results and Discussion

Figures 5 and 6 show the time dependence of the open circuit potential of the Pt disk electrode in 1 M $\rm H_2SO_4$ solution. The solid lines represent experimental data and the dotted lines the modeling data. The figures show the results for the modeling approach using solubility data. The same quality of fitting is obtained for both models of 'gas electrode' and 'flooded electrode'. It can be seen that the model, with it's assumption of first order reaction kinetics, fits very well for pure oxygen and air (Figures 5 and 6). In general, it can be observed that the final OCP value decreases with increasing temperature and decreasing oxygen concentration, as expected from theory.

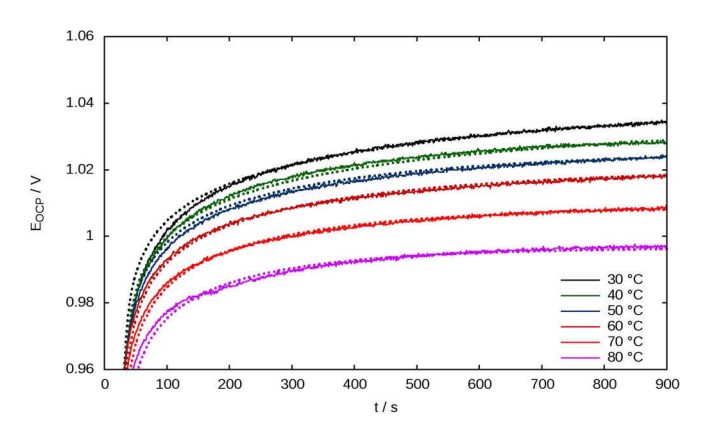


Figure 6. Time-dependence of the open circuit potential of Pt in 1 M H_2SO_4 in air. Straight lines = experiment and dotted lines = model from Equation 10.

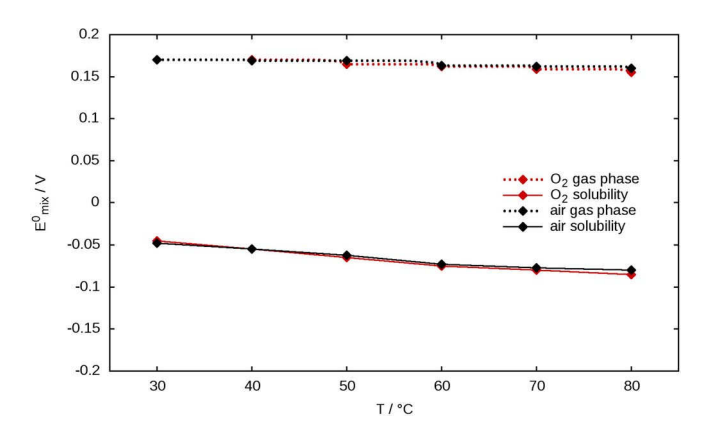


Figure 7. Mixed potential E_{mix}^0 as a function of temperature.

Figure 7 shows the resulting values of the fitting parameter $E_{mix}^0(T)$. From the theory, it can be concluded that standard potentials should not depend on concentration. Therefore, the results in Figure 7 are consistent because the same value is obtained for air and oxygen. The results only differ by the absolute value, which is caused by the difference of ≈ 200 mV between the model assumption of 'gas electrode' and 'flooded electrode'.

Figure 8 shows the resulting values for the reaction rate coefficient k as a function of temperature. The absolute value of k does not depend on the model approach for the Nernst equation. The rate constant k is higher for oxygen than for air. According to Equation 3 k should be independent of concentration. On the other hand, the water production reaction may be the driving force of the coupled reaction of platinum surface oxidation. A higher oxygen concentration would, in turn, provide 'more energy' and could increase the reaction rate.

The reaction rate constants can be interpreted as the surface fraction of the oxidized platinum species. Here, identical values of k result in identical values of surface fraction, as k and t are the only parameters in Equation 3. In Figure 9 the lowest value of S_{PtO} at $T=30^{\circ}\mathrm{C}$ and the highest value at $T=80^{\circ}\mathrm{C}$ are presented for oxygen and air. For oxygen, a comparably narrow range results and, after 900 s, the surface is almost completely oxidized. In the case of air, the temperature has a much stronger influence. At $T=80^{\circ}\mathrm{C}$ the surface becomes almost completely oxidized after 900 s, while for the lowest temperature $T=30^{\circ}\mathrm{C}$, a surface fraction of only 0.4 is reached.

It is interesting to take a closer look at the time-dependence of the OCP in air. From Figure 6, it can be determined that the OCP value changes rapidly within the first 100 s. After about 200 s, the value enters a region with a small linear-like slope. From this it can be determined that: after about three minutes, a fairly stable OCP

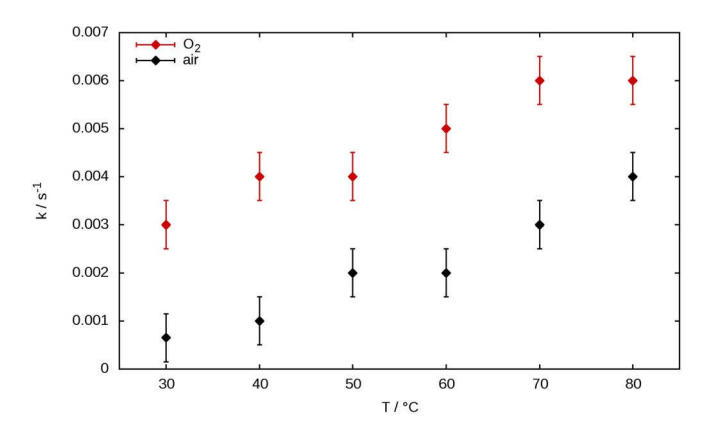


Figure 8. Reaction rate coefficient k as a function of temperature. The value of k does not depend on the approach for the Nernst equation. The error bars summarize all the uncertainty of the fitting process.

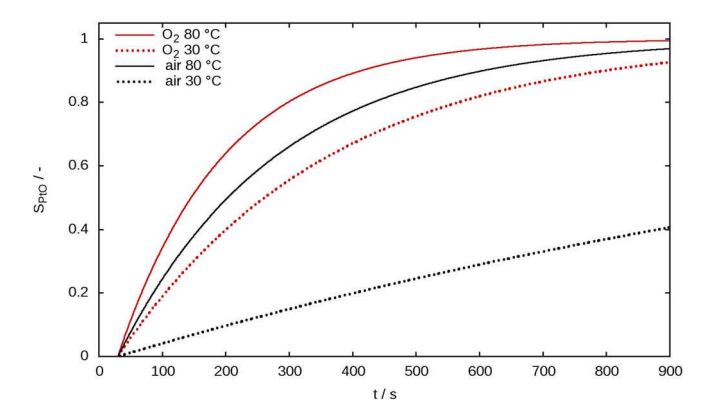


Figure 9. Surface coverage S_{PtO} as a function of time.

value is reached. At this time, up to 50% of the surface is covered by oxidized species. It could be said that the platinum surface is in an early state of oxygen adsorption and far from the region of surface layer reconstruction (see the sketch in Figure 3). The protocols for accelerated stress tests usually define potential cycling within a few seconds to upper potentials of 1.2 V or 1.4 V. It becomes obvious that in such cases, much higher degradation rates are to be expected. The influence of the upper potential limit on degradation rates was also proven experimentally. ^{47–49} It is shown that much lower degradation rates are observed if the upper potential is restricted to about 1.0 V.

In the case of oxygen the surface coverage is about 0.4 for $T=30^{\circ}\text{C}$ after 200 s. This value is fairly close to the value of 0.35, which was obtained from an early experiment by Hoare et al.⁴⁰

Conclusions

In this work, a macroscopic model was developed that describes the resulting open circuit potential of a polymer electrolyte fuel cell after a shut-down process. At an engineering level, the model aims to explain the principal influences on platinum surface oxidation. The theoretical work is supported by half-cell measurements of a platinum disk electrode. From the literature it is known that the difference between the theoretical Nernst potential and the open circuit voltage of a fuel cell can be explained by three effects: hydrogen cross-over, mixed catalyst potential and gas solubility in thin liquid films. The chosen experimental setup excludes the effect of hydrogen cross-over.

The results show that the time-dependence of the OCP value of the half cell can be explained by a first order growth mechanism of a platinum surface oxide layer. The model is in good agreement with measurements conducted in oxygen and air, which are the two most important gases for a fuel cell cathode. The contribution of the mixed catalyst potential to the Nernst equation seems to be almost independent of temperature in the range of 30°C to 80°C. The absolute value of E_{mix} depends on the physical model for the Nernst equation, namely the 'gas electrode' and 'flooded electrode'. The approach of the 'flooded electrode' yields a much closer match of the experimental values, but it is shown that the very popular approach of 'gas electrodes' can also be used.

The general conclusion from the model is that the growth of the surface oxide layer leads to a strong time-dependence within the first 200 s. After this period the OCP value may be approximated with the contribution of a static mixed potential. Interestingly, the resulting coverage of the catalyst with surface oxide ranges between 10% and 60% within the first 200 s. This might have a strong impact on the design of accelerated stress tests, as such tests commonly apply potentials that lead to a rigorous surface oxidation, including a restructuring of the catalyst surface. This impact should be examined in further detail. It is to be expected that the kinetics of surface oxidation of commercial fuel cell catalysts will be different, because small platinum particles in the nanometer range are used. Furthermore, the

effect of hydrogen crossover in real fuel cells will certainly influence the process of surface oxidation.

Another strong implication concerns the use of the Nernst equation in fuel cell modeling. The difference between OCP and the theoretical Nernst potential for the 'gas electrode' model leads to an offset that should be explicitly accounted for. Otherwise, the offset is distributed to other kinetic loss parameters, which in turn creates difficulties in the interpretation and comparison between different experiments.

Acknowledgment

Financial support from the Chinese Scholarship Council, grant numbers 201508610085 and 201508310123, is gratefully acknowledged by the authors.

ORCID

Uwe Reimer https://orcid.org/0000-0001-9776-8363
Yun Cai https://orcid.org/0000-0002-3407-8821
Ruiyu Li https://orcid.org/0000-0002-7116-8455
Dieter Froning https://orcid.org/0000-0003-2264-407X
Werner Lehnert https://orcid.org/0000-0002-7423-872X

References

- R. Borup, J. Meyers, B. Pivovar, Y. S. Kim, R. Mukundan, N. Garland, D. Myers, M. Wilson, F. Garzon, D. Wood, P. Zelenay, K. More, K. Stroh, T. Zawodzinski, J. Boncella, J. E. McGrath, M. Inaba, K. Miyatake, M. Hori, K. Ota, Z. Ogumi, S. Miyata, A. Nishikata, Z. Siroma, Y. Uchimoto, K. Yasuda, K.-I. Kimijima, and N. Iwashita, Scientific Aspects of Polymer Electrolyte Fuel Cell Durability and Degradation, *Chemical Reviews*, 107, 3904 (2007).
 S. Zhang, X.-Z. Yuan, J. N. C. Hin, H. Wang, K. A. Friedrich, and M. Schulze, A
- S. Zhang, X.-Z. Yuan, J. N. C. Hin, H. Wang, K. A. Friedrich, and M. Schulze, A review of platinum-based catalyst layer degradation in proton exchange membrane fuel cells, *J. Power Sources*, 194, 588 (2009).
- Y. Yu, H. Li, H. Wang, X.-Z. Yuan, G. Wang, and M. Pan, A review on performance degradation of proton exchange membrane fuel cells during startup and shutdown processes: Causes, consequences, and mitigation strategies, *J. Power Sources*, 205, 10 (2012).
- S. Cherevko, N. Kulyk, and K. J. J. Mayrhofer, Durability of platinum-based fuel cell electrocatalysts: Dissolution of bulk and nanoscale platinum, *Nano Energy*, 29, 275 (2016).
- J. P. Hoare, Rest potentials in the platinum-oxygen-acid system, J. Electrochem. Soc., 109, 858 (1962).
- H. Wroblowa, M. L. B. Rao, A. Damjanovic, and J. O'M. Bockris, Adsorption and kinetics at platinum electrodes in the presence of oxygen at zero net current, *J. Electroanal. Chem.*, 15, 139 (1967).
- R. Thacker and J. P. Hoare, Sorption of oxygen from solution by noble metals I. Bright platinum, *J. Electroanal. Chem.*, 30, 1 (1971).
- M. Whitfield, Thermodynamic limitations on the use of the platinum electrode in Eh measurements, *Limnol. Oceanogr.*, 19, 857 (1974).
- J. Zhang, Y. Tang, C. Song, J. Zhang, and H. Wang, PEM fuel cell open circuit voltage (OCV) in the temperature range of 23°C to 120°C, J. Power Sources, 163, 532 (2006).
- U. Reimer, W. Lehnert, Y. Holade, and B. Kokoh, Irreversible losses in fuel cells. In Fuel Cells and Hydrogen - From Fundamentals to Applied Research, V. Hacker and S. Mitsushima, editors, 15–40. Elsevier (2018).
- Z. Qi, Proton exchange membrane fuel cells. CRC Press, Boca Raton, London, New York, (2014).
- M. G. Santarelli, M. F. Torchio, and P. Cochis, Parameters estimation of a PEM fuel cell polarization curve and analysis of their behavior with temperature, *J. Power Sources*, 159, 824 (2006).
- J. Kim, S. M. Lee, S. Srinivasan, and C. E. Chamberlin, Modeling of proton exchange membrane fuel cell with an empirical equation, *J. Electrochem. Soc.*, 142, 2670 (1995)
- S. A. Vilekar and R. Datta, The effect of hydrogen crossover on open-circuit voltage in polymer electrolyte membrane fuel cells, J. Power Sources, 195, 2241 (2010).
- C. Song, Y. Tang, J. L. Zhang, J. Zhang, H. Wang, J. Shen, S. McDermid, J. Li, and P. Kozak, PEM fuel cell reaction kinetics in the temperature range of 23–120°C, *Electrochim. Acta*, 52, 2552 (2007).
- A. Parthasarathy, S. Supramaniam, A. J. Appleby, and C. R. Martin, Temperature dependence of the electrode kinetics reduction at the platinum/Nafion interface - a microelectrode investigation. *J. Electrochem. Soc.*, 139, 2530 (1992).
- R. Petrone, D. Hissel, M. C. Péra, D. Chamagne, and R. Gouriveau, Accelerated stress test procedures for PEM fuel cells under actual load constraints: State-of-art and proposals, *Int. J. Hydrogen Energy*, 40, 12489 (2015).
- S. Zhang, X. Yuan, H. Wang, W. Mérida, H. Zhu, J. Shen, S. Wu, and J. Zhang, A review of accelerated stress tests of MEA durability in PEM fuel cells, *Int. J. Hydrogen Energy*, 34, 388 (2009).
- R. P. O'Hayre, S.-W. Cha, W. G. Colella, and F. B. Prinz, Fuel Cell Fundamentals. Wiley, New York, 2 edition, (2009).

- 20. F. Barbir, PEM Fuel Cells. Elsevier, Amsterdam, Boston, Heidelberg, (2005).
- A. A. Kulikovsky, Analytical Modelling of Fuel Cells. Elsevier, Amsterdam, Boston, Heidelberg, (2010).
- M. Peuckert and H. P. Bonzel, Effect of oxide thickness on the rates of some redox reactions on a platinum electrode, *Surf. Sci.*, 145, 239 (1984).
- A. T. Kuhn and T. H. Randle, Effect of oxide thickness on the rates of some redox reactions on a platinum electrode, J. Chem. Soc., Faraday Trans. 1, 81, 403 (1985).
- L. D. Burke, J. J. Borodzinski, and K. J. O'Dwyer, Multilayer oxide growth on platinum under potential cycling conditions – I sulphuric acid solution. *Electrochim. Acta*, 35, 967 (1990).
- L. D. Burke and K. J. O'Dwyer, Multilayer oxide growth on Pt under potential cycling conditions – II HClO₄ and NaOH solutions, *Electrochim. Acta*, 37, 43 (1992).
- L. D. Burke and D. T. Buckley, Anomalous stability of acid-grown hydrous platinum oxide films in aqueous media, *J. Electroanal. Chem.*, 366, 239 (1994).
- P. Vanýsek, Electrochemical series. In CRC Handbook of Chemistry and Physics, D. R. Lide, editor, 8–21. CRC Press, Boca Raton, Boston, London, New York79 edition (1998).
- H. Angerstein-Kozlowska, B. E. Conway, and W. B. A. Sharp, The real condition of electrochemically oxidized platinum surfaces, Part I: Resolution of component processes, J. Electroanal. Chem. Interfacial Electrochem., 43, 9 (1973).
- B. E. Conway and S. Gottesfeld, Real condition of oxidized platinum electrodes. Part
 Resolution of reversible and irreversible processes by optical and impedance studies, J. Chem. Soc., Faraday Trans. 1, 69, 1090 (1973).
- B. V. Tilak, B. E. Conway, and H. Angerstein-Kozlowska, The real condition of oxidized Pt electrodes, Part III: Kinetic theory of formation and reduction of surface oxides, *J. Electroanal. Chem. Interfacial Electrochem.*, 48, 1 (1973).
- G. Jerkiewicz, G. Vatankhah, J. Lessard, M. P. Sriaga, and Y.-S. Park, Surfaceoxide growth at platinum electrodes in aqueous H₂SO₄ Reexamination of its mechanism through combined cyclic-voltammetry, electrochemical quartz-crystal nanobalance, and Auger electron spectroscopy measurements, *Electrochim. Acta*, 49, 11451 (2004)
- J. Drnec, D. A. Harrington, and O. M. Magnussen, Electrooxidation of Pt (111) in acid solution, Curr. Opin. Electrochem., 4, 69 (2017).
- J. Drnec, M. Ruge, F. Reikowski, B. Rahn, F. Carlá, R. Felici, J. Stettner, O. M. Magnussen, and D. A. Harrington, Initial stages of Pt(111) electrooxidation: dynamic and structural studies by surface X-ray diffraction, *Electrochim. Acta*, 224, 220 (2017).
- A. M. Gómez-Marín, J. Clavilier, and J. M. Feliu, Sequential Pt(111) oxide formation in perchloric acid: an electrochemical study of surface species inter-conversion, J. Electroanal. Chem., 688, 360 (2013).

- B. E. Conway, Electrochemical oxide film formation at noble metals as a surfacechemical process, *Prog. Surf. Sci.*, 49, 331 (1995).
- N. A. Anastasijević, V. Vesović, and R. R. Adžić, Determination of the kinetic parameters of the oxygn reduction reaction using the rotating ring-disk electrode, Part I Theory, J. Electroanal. Chem., 229, 305 (1987).
- Z. Nagy and H. You, Applications of surface X-ray scattering to electrochemistry problems, *Electrochim. Acta*, 47, 3037 (2002).
- E. F. Holby and D. Morgan, Application of Pt Nanoparticle Dissolution and Oxidation Modeling to Understanding Degradation in PEM Fuel Cells, *J. Electrochem. Soc.*, 159, B578 (2012).
- R. M. Darling and J. P. Meyers, Kinetic model of platinum dissolution in PEMFCs, J. Electrochem. Soc., 150, A1523 (2003).
- J. P. Hoare, R. Thacker, and C. R. Wiese, Sorption of oxygen from solution by noble metals - II. Nitric acid-passivated bright platinum, *J. Electroanal. Chem.*, 30, 15 (1971).
- V. Weissbecker, U. Reimer, K. Wippermann, and W. Lehnert, A Comprehensive Corrosion Study on Metallic Materials for HT-PEFC Application, *ECS Trans.*, 58, 693 (2013).
- V. Weissbecker, K. Wippermann, and W. Lehnert, Electrochemical Corrosion Study of Metallic Materials in Phosphoric Acid as Bipolar Plates for HT-PEFCs, *J. Electrochem. Soc.*, 161, F1437 (2014).
- Y. Garsany, O. A. Baturina, K. E. Swider-Lyons, and S. S. Kocha, Experimental Methods for Quantifying the Activity of Platinum Electrocatalysts for the Oxygen Reduction Reaction. *Analytical Chemistry*, 82, 6321 (2010).
- NIST National Institute of Standards and Technology. NIST Chemistry Webbook, Water. https://webbook.nist.gov, (2018).
- L. H. Gevantmann, Solubility of selected gases in water. In CRC Handbook of Chemistry and Physics, D. R. Lide, editor, 8–86. CRC Press, Boca Raton, Boston, London, New York79 edition (1998).
- L. V. Gurvich, V. S. Iorish, V. S. Yungman, and O. V. Dorofeeva, Thermodynamic properties as a function of temperature. In *CRC Handbook of Chemistry and Physics*, D. R. Lide, editor, 5–61. CRC Press, Boca Raton, Boston, London, New York79 edition (1998).
- K. Kinoshita, J. T. Lundquist, and P. Stonehart, Potential cycling effects on platinum electrocatalyst surfaces, *J. Electroanal. Chem. Interfacial Electrochem.*, 48, 157 (1973)
- R. L. Borup, J. R. Davey, F. H. Garzon, D. L. Wood, and M. A. Inbody, PEM fuel cell electrocatalyst durability measurements, *J. Power Sources*, 163, 76 (2006).
- A. Marcu, G. Toth, and R. J. Behm, Electrochemical test procedures for accelerated evaluation of fuel cell cathode catalyst degradation, *Fuel Cells*, 14, 378 (2014).